Photoinduced Electron Transfer in Supramolecular Assemblies Composed of Alkoxyanisyl-Tethered Ruthenium(II)−Tris(bipyridazine) Complexes and a Bipyridinium Cyclophane Electron Acceptor

Marlene Kropf,[1] Ernesto Joselevich,[2] Heinz Dürr,[1] and Itamar Willner*[,2]

Contribution from the Universität des Saarlandes, Organische Chemie, Fachbereich 11.2, 66041 Saarbrücken, Germany, and The Institute of Chemistry and the Farkas Center for Light Induced Processes, The Hebrew University of Jerusalem, Jerusalem 91904, Israel

Received June 26, 1995[⊗]

Abstract: Photoinduced electron transfer in photosystems consisting of bis(6,6′-dimethoxy-3,3′-bipyridazine)(6,6′-bis[8-((4-methoxyphenyl)oxy)-3,6-dioxaoctyl-1-oxy]-3,3′-bipyridazine)ruthenium(II) dichloride (**1**), tris(6,6′-bis[8-((4-methoxyphenyl)oxy)-3,6-dioxaoctyl-1-oxy]-3,3′-bipyridazine)ruthenium(II) dichloride (**2a**), tris(6,6′-bis[11-(4-methoxyphenyl)-3,6,9-trioxa-undecyl-1-oxy]-3,3′-bipyridazine)ruthenium(II) dichloride (**2b**), and tris(6-(8-hydroxy-3,6-dioxa-octane-1-oxy)-6′-[8-((4-methoxyphenyl)oxy)-3,6-dioxaoctyl-1-oxy]-3,3′-bipyridazine)-1,3,5-benzenetricarboxylate-ruthenium(II) dichloride (**3**), with bis(*N*,*N*′-*p*-xylylene-4,4′-bipyridinium) (BXV^{4+}, **4**) were examined. The series of photosensitizers include alkoxyanisyl donor components tethered to the photosensitizer sites, capable of generating donor−acceptor supramolecular complexes with BXV^{4+} (**4**). Detailed analyses of the steady-state and time-resolved electron transfer quenching reveal a rapid intramolecular electron transfer quenching, k_{sq}, within the supramolecular assemblies formed between the photosensitizers and BXV^{4+} (**4**) and a diffusional quenching, k_{dq}, of the free photosensitizers by BXV^{4+} (**4**). A comprehensive model that describes the electron transfer in the different photosystems and assumes the formation of supramolecular assemblies of variable stoichiometries, SA_n, is formulated. Analysis of the experimental results according to the formulated model indicates that supramolecular complexes between **1**−**3** and BXV^{4+} of variable stoichiometries exist in the different photosystems. Maximal supramolecular stoichiometries between **1**, **2a** and **3**, and BXV^{4+} (**4**), corresponding to $N = 2$, 6, and 3, respectively, contribute to the electron transfer quenching paths. The derived association constants of BXV^{2+} to a single binding site in the photosensitizers **1**, **2a**, **2b**, and **3** are 240, 100, 100, and 140 M^{-1}, respectively. The back electron transfer of the photogenerated redox products was followed in the different photosystems. Back electron transfer proceeds via two routes that include the intramolecular recombination, k_{sr}, within the supramolecular diads and diffusional recombination, k_{dr}, of free redox photoproducts. Detailed analysis of the back electron transfer in the different photosystems revealed that the non-covalently linked supramolecular assemblies, SA_n, act as static diads where electron-transfer quenching and recombination occurs in intact supramolecular structures despite the dynamic nature of the systems. The lifetime of the redox photoproducts $Ru^{3+}-BXV^{\bullet 3+}$ in the various systems is relatively long as compared to diad assemblies (0.56−1.20 μs). This originates from electrostatic repulsive interactions of the photoproducts within the supramolecular assemblies resulting in stretched conformations of the diads and spatial separation of the redox products.

Introduction

Substantial efforts are directed toward mimicking the vectorial electron-transfer and charge separation in the photosynthetic reaction center.[3] Electron transfer in covalently linked donor−acceptor diads,[4] triads,[5,6] and pentads[7] was extensively studied, and effective stabilization of the electron transfer products was accomplished by the vectorial spatial separation of the redox products in the molecular arrays. Further stabilization of the redox products in molecular triads was achieved by coupling the molecular assemblies to heterogeneous matrices,[8] i.e. zeolites[8a] or layered phosphates.[8b] In these systems, structured alignment and rigidification of the molecular systems result in

* To whom correspondence should be addressed.

⊗ Abstract published in *Advance ACS Abstracts,* January 1, 1996.

(1) Universität des Saarlandes, Organische Chemie, Fachbereich 11.2, 66041 Saarbrücken, Germany.

(2) Institute of Chemistry, The Hebrew University of Jerusalem, Jerusalem 91904, Israel. Fax: 972-2-6527715

(3) (a) Deisenhofer, J.; Epp, O.; Miki, K.; Huber, R.; Michel, H. *J. Mol. Biol.* **1984**, *180*, 385. (b) Deisenhofer, J.; Epp, O.; Miki, K.; Huber, R.; Michel, H. *Nature* **1985**, *318*, 618. (c) Chang, C. H.; Tiede, D.; Tang, J.; Smith, U.; Norris, J.; Schiffer, M. *FEBS Lett.* **1986**, *205*, 82.

(4) (a) Connolly, J. S.; Bolton, J. R. In *Photoinduced Electron Transfer, Part D*; Fox, M. A., Chanon, M., Eds.; Elsevier: Amsterdam, Section 6.2. (b) Cooley, L. F.; Headford, C. E. L.; Elliott, C. M.; Kelley, D. F. *J. Am. Chem. Soc.* **1988**, *110*, 6673.

(5) (a) Gust, D.; Moore, T. A. *Top. Curr. Chem.* **1991**, *159*, 103. (b) Gust, D.; Moore, T. A. *Science* **1989**, *244*, 35. (c) Moore, T. A.; Gust, D.; Moore, A. L.; Bensasson, R. V.; Seta, P.; Bienvenue, E. In *Supramolecular Photochemistry*; Balzani, V., Ed.; D. Reidel: Boston, 1987; p 283. (d) Gust, D.; Moore, T. A. In *Supramolecular Photochemistry*; Balzani, V., Ed.; D. Reidel: Boston, 1987; p 267. (e) Wasielewski, M. R.; Gains, G. L., III; Wiederrecht, G. P.; Svec, W. A.; Niemczyk, M. P. *J. Am. Chem. Soc.* **1993**, *115*, 10442.

(6) (a) Sanders, G. M.; van Dijk, M.; van Veldhuizen, A.; van der Plas, M. J. *J. Chem. Soc., Chem. Commun.* **1986**, 1311. (b) Wasielewski, M. R.; Niemczyk, M. P.; Svec, W. A.; Pewitt, E. B. *J. Am. Chem. Soc.* **1985**, *107*, 5562. (c) Mecklenburg, S. L.; Peek, B. M.; Erickson, B. W.; Meyer, T. J. *J. Am. Chem. Soc.* **1987**, *109*, 3297. (d) Danielson, E.; Elliott, C. M.; Mesket, J. W.; Meyer, T. J. *J. Am. Chem. Soc.* **1987**, *109*, 2519. (e) Johnson, D. G.; Niemczyk, M. P.; Minsek, D. W.; Widerrecht, G. P.; Svec, W. A.; Gaines, G. L., III; Wasielewski, M. R. *J. Am. Chem. Soc.* **1993**, *115*, 5692.

(7) (a) Kurreck, H.; Huber, M. *Angew. Chem., Int. Ed. Engl.* **1995**, *34*, 849. (b) Gust, D.; Moore, T. A.; Moore, A. L.; Lee, S.-J.; Bittersmann, E.; Luttrull, D. K.; Rehms, A. A.; DeGraziano, J. M.; Ma, X. C.; Gao, F.; Belfored, R. E.; Trier, T. T. *Science* **1990**, *248*, 199.

0002-7863/96/1518-0655$12.00/0

the stabilization of the redox products against back electron transfer. A further method to organize photosensitizer−acceptor diads involved intermolecular non-covalent linkage of the diad components by complementary H bonds or a molecular receptor unit.[9,10] Recently, we reported on a novel approach to organize chromophore−electron acceptor diad assemblies by the application of electron donor-modified chromophores that form the supramolecular non-covalently-linked diads with the electron acceptor via donor−acceptor interactions.[11] Similarly, we showed that the formation of donor−acceptor supramolecular complexes between a molecular triad and electron donor results in steric rigidification of the triad that results in photoinduced vectorial electron transfer and stabilization of the redox products against back electron transfer.[12]

It is established that *N*,*N*′-dialkylbipyridinium salts form donor-acceptor complexes with different electron donors.[13,14] Recently, the intermolecular complexes between dialkoxybenzenes and cyclo[bis(*N*,*N*′-*p*-xylylene-4,4′-bipyridinium)], BXV^{4+}, were extensively studied by Stoddart and co-workers.[15,16] It was found that dialkoxybenzene intercalates into the bipyridinium cyclophane via donor−acceptor interaction, and the resulting stable supramolecular assemblies were applied to synthesize ingenious catenane macromolecules.[17,18] Chemical modification of Ru(II)−polypyridine complexes with dialkoxybenzene units could provide binding sites for the BXV^{4+} electron acceptor. Here we wish to report on the supramolecular complexes formed between the series of alkoxyanisyl-tethered Ru(II)−tris(bipyridazine) complexes: bis(6,6′-dimethoxy-3,3′-bipyridazine)(6,6′-bis[8-((4-methoxyphenyl)oxy)-3,6-dioxaoctyl-1-oxy]-3,3′-bipyridazine)ruthenium(II) dichloride (**1**), tris(6,6′-bis[8-((4-methoxyphenyl)oxy)-3,6-dioxaoctyl-1-oxy]-3,3′-bipyridazine)ruthenium(II) dichloride (**2**), and tris(6-(8-hydroxy-3,6-dioxaoctyl-1-oxy)-6′-[8-((4-methoxyphenyl)oxy)-3,6-dioxaoctyl-1-oxy]-3,3′-bipyridazine)-1,3,5-benzene-tricarboxylate-ruthenium(II) dichloride (**3**), with the bipyridinium cyclophane (BXV^{4+}, **4**). We examine the electron-transfer quenching pathways in the resulting supramolecular assemblies and characterize the resulting photogenerated redox products and their recombination in the supramolecular assemblies. We find that effective electron-transfer quenching of the excited chromophores proceeds in the supramolecular systems and that the resulting supramolecular complex of photoproducts is preserved. We reveal that the lifetime of the photogenerated redox products in the supramolecular asemblies is long as compared to other molecular diad systems. This is attributed to the fact that the alkoxyanisyl binding sites are tethered to the Ru(II) chromophores by poly(ethylene glycol) chains. Association of BXV^{4+} to the binding sites results in electrostatic repulsions between the electron-acceptor and the Ru(II)-chromophore component that induce the steric spatial separation of the redox products which are stabilized against back electron transfer.

Experimental Section

Absorption spectra were recorded with a Uvikon-860 (Kontron) spectrophotometer. Fluorescence spectra were recorded with a SFM-25 (Kontron) spectrofluorometer. Flash photolysis experiments were carried out with a Nd-YAG laser (Model GCR-150, Spectra Physics) coupled to a detection system (Applied Photophysics K-347) that included a monochromator and photomultiplier linked to a digitizer (Tektronix 2430 A) and computer for data storage and processing. This flash-photolysis setup has a time resolution of >20 ns. For shorter time-scale transients (>0.5 ns) a flash photolysis system consisting of a N_2 laser (PRA, LN-1000) coupled to a dye laser (Laser Photonics, Coumarin 440) was employed. These lasers were coupled to a detection system consisting of a monochromator and photomultiplier (Applied Photophysics) linked to a digitizer (Tektronix 7912 AD) and a computer for data storage and analysis.

All materials and solvents were of highest purity from commercial sources (Aldrich, Sigma). The ligands (6,6′-bis[8-((4-methoxyphenyl)-oxy)-3,6-dioxaoctyl-1-oxy]-3,3′-bipyridazine and (6,6′-bis[8-((4-methoxyphenyl)oxy)-3,6,9-trioxaundecyl-1-oxy]-3,3′-bipyridazine were prepared by coupling[19,20] of 6-[8-((4-methoxyphenyl)oxy)-3,6-dioxaoctyl-1-oxy)-3-chloropyridazine or 6-[11-((4-methoxyphenyl)oxy)-3,6-trioxaundecyl-1-oxy]-3-chloropyridazine, respectively, in the presence of $Ni(PPh_3)_4$ (DMF, 8h) followed by chromatographic purification (SiO_2, $CH_2Cl_2-CH_3OH$ 95:5 (v/v) as eluent). The photosensitizer bis-(6,6′-dimethoxy-3,3′-bipyridazine)(6,6′-bis[8-((4-methoxyphenyl)oxy)-3,6-dioxaoctyl-1-oxy)-3,3′-bipyridazine)ruthenium(II) dichloride (**1**) was prepared by the reaction of Ru(II)-bis(6,6′-dimethoxy-3,3′-bipyridazine) (100 mmol) and the respective ligand (150 mmol) (ethylene glycol, 180 °C, 4 h) followed by chromatographic separation (SiO_2, $CH_2Cl_2-CH_2OH$ 80:20 (v/v) as eluent). The photosensitizers, tris(6,6′-bis[8-((4-methoxyphenyl)oxy)-3,6-dioxaoctyl-1-oxy]-3,3′-bipyridazine)ruthenium(II) dichloride (**2a**) and tris(6,6′-bis[11-((4-methoxyphenyl)oxy)-3,6,9-trioxaundecyl-1-oxy]-3,3′-bipyridazine)ruthenium(II) dichloride (**2b**), were prepared by the reaction of $Ru(DMSO)_4Cl_2$ (100 mmol) and the respective ligands (400 mmol) in ethanol−H_2O, 3:1 (v/v) (reflux, 24 h), followed by chromatographic purification (SiO_2, $CH_2Cl_2-CH_3OH$, 80:20 (v/v) as eluent).

The ligand (6-[3,6-dioxaoctyl-1-oxy]-6′-[8-((4-methoxyphenyl)oxy)-3,6-dioxaoctyl-1-oxy]-3,3′-bipyridazine)-1,3,5-benzene-tricarboxylate was prepared by the reaction between 6-(8-hydroxy-3,6-dioxaoctyl-1-oxy)-6′-[8-((4-methoxyphenyl)oxy)-3,6-dioxaoctane and benzene tri-

(8) (a) Yonemoto, E. H.; Kim, Y. I.; Schmehl, R. H.; Wallis, J. O.; Shoulders, B. A.; Richardson, B. R.; Haw, J. F.; Mallouk, T. E. *J. Am. Chem. Soc.* **1994**, *116*, 10557. (b) Vermuelen, L. A.; Thompson, M. E. *Nature* **1992**, *358*, 656. (c) Ungashe, S. B.; Wilson, W. L.; Katz, H. E.; Scheller, G. R.; Putrinski, T. M. *J. Am. Chem. Soc.* **1992**, *114*, 8717.

(9) (a) Sessler, J. L.; Wang, B.; Harriman, A. *J. Am. Chem. Soc.* **1993**, *115*, 10418. (b) Harriman, A.; Kubo, Y.; Sessler, J. L. *J. Am. Chem. Soc.* **1992**, *114*, 388. (c) Turró, C.; Chang, C. K.; Leroi, G. E.; Cukier, R. I.; Nocera, D. G. *J. Am. Chem. Soc.* **1992**, *114*, 4013.

(10) (a) Sun, L.; von Gersdorff, J.; Niethammer, D.; Tian, P.; Kurreck, H. *Angew. Chem., Int. Ed. Engl.* **1994**, *33*, 2318. (b) Sun, L.; von Gersdorff, J.; Sobek, J.; Kurreck, H. *Tetrahedron* **1995**, *51*, 3535. (c) Dürr, H.; Bossmann, S.; Schwarz, R. *J. Inf. Rec. Mater.* **1994**, *21*, 471. (d) Dürr, H.; Bossmann, S.; Kropf, M.; Hayo, R.; Turro, N. J. *J. Photochem. Photobiol. A: Chemistry* **1994**, *80*, 341.

(11) Seiler, M.; Dürr, H.; Willner, I.; Joselevich, E.; Doron, A.; Stoddart, J. F. *J. Am. Chem. Soc.* **1994**, *116*, 3399.

(12) Zahavy, E.; Seiler, M.; Marx-Tibbon, S.; Joselevich, E.; Willner, I.; Dürr, H.; O'Connor, D.; Harriman, A. *Angew. Chem., Int. Ed. Engl.* **1995**, *34*, 1005.

(13) (a) Willner, I.; Eichen, Y.; Rabinovitz, M.; Hoffman, R.; Cohen, S. *J. Am. Chem. Soc.* **1992**, *114*, 637. (b) Kisch, H.; Fernandez, A.; Wakatsuki, Y.; Yamazaki, H. *Z. Naturforsch.* **1985**, *406*, 292. (c) Nakamura, K.; Kai, Y.; Yasuoka, N.; Kasai, N. *Bull. Chem. Soc. Jpn.* **1981**, *54*, 3300.

(14) (a) Usui, Y.; Misawa, H.; Sakuragi, H.; Tokumara, U. *Bull. Chem. Soc. Jpn.* **1987**, *60*, 1573. (b) Willner, I.; Eichen, Y.; Joselevich, E. *J. Phys. Chem.* **1990**, *94*, 3092.

(15) Anelli, P. L.; Ashton, P. R.; Ballardini, R.; Balzani, V.; Delgado, M.; Gandolfi, M. T.; Goodnow, T. T.; Kaifer, A. E.; Philip, D.; Pietraszkiewicz, M.; Prodi, L.; Reddington, M. V.; Slavin, A. M. Z.; Spencer, N.; Stoddart, J. F.; Vincent, C.; Williams, D. J. *J. Am. Chem. Soc.* **1992**, *114*, 193.

(16) (a) Anelli, P. L.; Ashton, P. R.; Spencer, N.; Slawin, A. M. Z.; Stoddart, J. F.; Williams, D. J. *Angew. Chem., Int. Ed. Engl.* **1991**, *30*, 1036. (b) Ashton, P. R.; Odell, B.; Reddington, M. V.; Slavin, A. M. Z.; Stoddart, J. F.; Williams, D. J. *Angew. Chem.* **1988**, *27*, 1550.

(17) (a) Anelli, P. L.; Spencer, N.; Stoddart, J. F. *J. Am. Chem. Soc.* **1991**, *113*, 5131. (b) Ashton, P. R.; Brown, C. L.; Chrystal, E. J. T.; Goodnow, T. T.; Kaifer, A. E.; Parry, K. P.; Slawin, A. M. Z.; Spencer, N.; Stoddart, J. F.; Williams, D. J. *Angew. Chem., Int. Ed. Engl.* **1991**, *30*, 1039. (c) Ashton, P. R.; Philip, D.; Spencer, N.; Stoddart, J. F. *J. Chem. Soc., Chem. Commun.* **1992**, 1124.

(18) (a) Bissell, R. A.; Cordova, E.; Kaifer, A. E.; Stoddart, J. F. *Nature* **1994**, *369*, 133. (b) Ashton, P. R.; Ballardini, R.; Balzani, V.; Gandolfi, M. T.; Marquis, D. J.-F.; Peréz-Garciá, L.; Prodi, L.; Stoddart, J. F.; Venturi, M. *J. Chem. Soc., Chem. Commun.* **1994**, 177. (c) Amabilino, D. B.; Ashton, P. R.; Reder, A. S.; Spencer, N.; Stoddart, J. F. *Angew. Chem., Int. Ed. Engl.* **1994**, *33*, 433.

(19) (a) Tiecco, M. *Bull. Soc. Chim. Belg.* **1986**, *95*, 1009. (b) Kendo, A.; Liebeskind, L.; Braitsch, D. *Tetrahedron Lett.* **1975**, 3375.

(20) Detailed synthesis of the complexes will be described elsewhere: Dürr, H.; Kropf, M. In preparation.

Chart 1

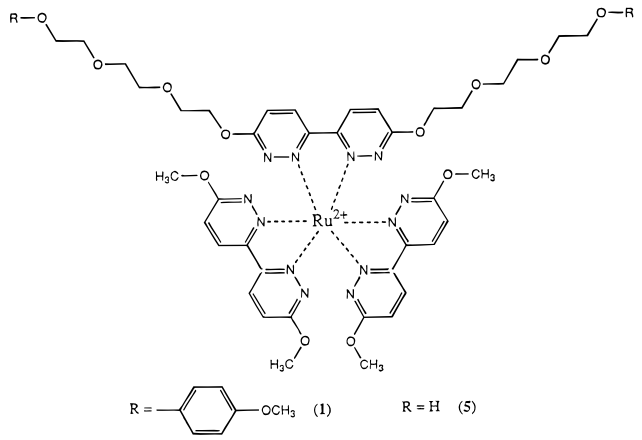

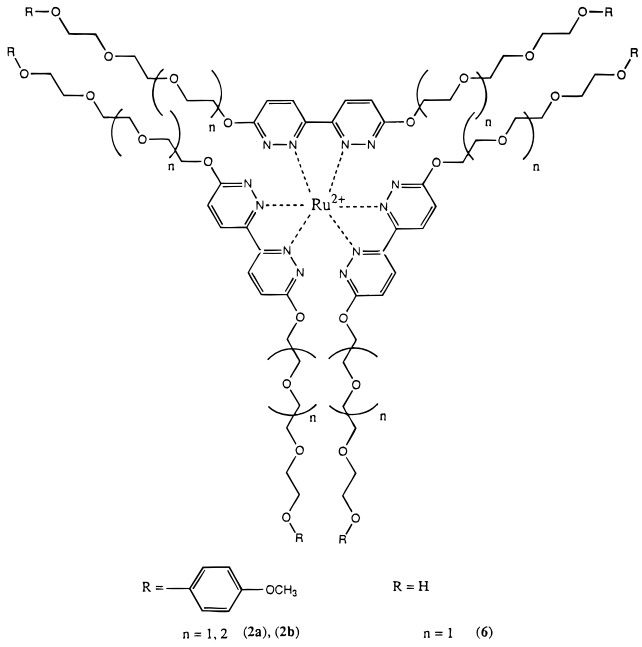

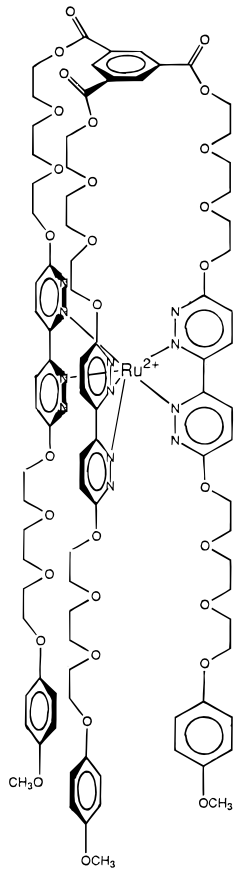

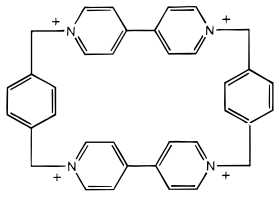

carboxychloride.[18] The photosensitizer tris(6-(8-hydroxy-3,6-dioxaoctyl-1-oxy)-6′-[8-((4-methoxyphenyl)oxy)-3,6-dioxaoctyl-1-oxy]-3,3′-bipyrazidine)-1,3,5-benzene-tricarboxylate-ruthenium(II) dichloride (**3**) was prepared by the reaction of the latter ligand (100 mmol) with Ru(DMSO)$_4$Cl$_2$ (100 mmol) in ethanol−H_2O, 3:1 (v/v) (reflux, 24 h) followed by chromatographic purification (Sephadex G-15, H_2O as eluent). The ligands 6,6′-bis[8-hydroxy-3,6-dioxaocttl-1-oxy]-3,3′-bipyridazine and 6,6′-bis[11-hydroxy-3,6,9-trioxaundecyl-1-oxy]-3,3′-bipyridazine were prepared by coupling[19] of 6-[8-hydroxy-3,6-dioxaoctyl-1-oxy]-3-chloropyridazine or 6-[11-hydroxy-3,6,9-trioxaundecyl-1-oxy]-3-chloropyridazine (DMF, 8 h) followed by chromatographic purification (SiO_2, CH_2Cl_2−CH_3OH, 90:10 (v/v) as eluent). The photosensitizer bis(6,6′-dimethoxy-3,3′-bipyridazine)(6,6′-bis[8-hydroxy-3,6-dioxaoctyl-1-oxy]-3,3′-bipyridazine)ruthenium(II) dichloride (**5**) was prepared by the reaction of Ru(II)-bis(6,6′-bis(methoxy))-3,3′-bipyridazine (100 mmol) and the latter ligand (150 mmol) (ethylene glycol, 180 °C, 4 h) followed by chromatographic separation (Sephadex G10, water as eluent). Cyclo[bis(*N*,*N*′-*p*-xylylene-4,4′-bipyridinium)] tetrachloride (**4**) was prepared according to the literature.[21] All compounds gave satisfactory elementary analyses and ^{1}H-NMR spectra.

All photochemical measurements were performed in triply distilled water.All steady-state fluorescence and time-resolved quenching experiments were performed in 0.4 × 1 cm glass cuvettes that included an aqueous solution of the respective photosensitizer, 4.0×10^{-5} M (O.D. $\approx$ 1.0), and the appropriate concentration of the BXV^{4+}. In steady-state experiments $\lambda_{ex} = 460$ nm, and in the transient experiments using the Nd-Yag laser $\lambda_{ex} = 532$ nm and for the N_2-dye laser $\lambda_{ex} = 437$ nm. The resulting emission was recorded at $\lambda_{em} = 600$ nm. The recombination processes were characterized in aqueous solution that included the respective photosensitizer, 4.0×10^{-5} M, and BXV^{4+}, 4.36×10^{-3} M. All transient measurements were performed under an oxygen-free Ar atmosphere.

Results and Discussion

The electron-transfer quenching and charge separation in a series of supramolecular systems consisting of polyethylene oxyanisyl Ru(II)-bipyridazine complexes, acting as photosensitizers, and *N*,*N*′-bipyridinium salts acting as electron acceptors were examined. The photosensitizer series include bis(6,6′-dimethoxy-3,3′-bipyridazine)(6,6′-bis[8-((4-methoxyphenyl)-oxy)-3,6-dioxaoctyl-1-oxy]-3,3′-bipyridazine)ruthenium(II) dichloride (**1**), tris(6,6′-bis[8-((4-methoxyphenyl)oxy)-3,6-dioxaoctyl-1-oxy]-3,3′-bipyridazine)ruthenium(II) dichloride (**2a**), tris(6,6′-bis[11-((4-methoxyphenyl)oxy)-3,6,9-trioxaundecyl-1-oxy]-3,3′-bipyridazine)ruthenium(II) dichloride (**2b**), and tris(6-(8-hydroxy-3,6-dioxaoctyl-1-oxy)-6′-[8-((4-methoxyphenyl)oxy)-3,6-

(21) Odell, B.; Reddington, M. V.; Slawin, A. M. Z.; Spencer, N.; Stoddart, J. F.; Williams, D. J. *Angew. Chem., Int. Ed. Engl.* **1988**, *27*, 1547.

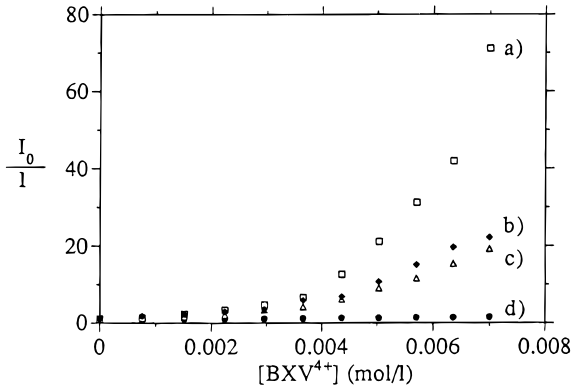

Figure 1. Steady-state luminescence quenching of (a) **2a**, (b) **3**, (c) **1**, and (d) **6**. All photosensitizers are at a concentration corresponding to 4×10^{-5} M.

dioxaoctyl-1-oxy]-3,3′-bipyridazine)-1,3,5-benzene-tricarboxylate-ruthenium(II) dichloride (**3**). All of the Ru(II)−bipyridazine complexes include *p*-methoxyanisyl units that form charge-transfer complexes with bis(*N*,*N*′-(*p*-xylylene)-4,4′-bipyridinium (BXV^{4+}, **4**). The formation of charge-transfer supramolecular complexes between 1,4-dimethoxybenzene and the bis-bipyridinium cyclophane, BXV^{4+} (**4**), has been specifically demonstrated by Stoddart and co-workers in recent years. Photoinduced electron transfer from Ru(II)−polypyridine complexes to bipyridinium electron acceptors has been studied extensively. Thus, formation of photosensitizer/electron acceptor complexes between the *p*-methoxyanisyl units linked to the Ru(II)−bipyridazine complexes (**1**−**3**) is anticipated to control the photoinduced electron transfer in the resulting supramolecular assemblies.

Figure 1 shows the steady-state luminescence quenching of the series of complexes **1**−**3** by BXV^{4+} (**4**). Nonlinear Stern−Volmer plots are obtained for all of the photosensitizers and the highest deviation from linearity is observed for **2**. As control experiments, the luminescence quenching processes of the photosensitizers bis(6,6′-dimethoxy-3,3′-bipyridazine)(6,6′-bis-[8-hydroxy-3,6-dioxaoctyl-1-oxy]-3,3′-bipyridazine)ruthenium-(II) dichloride (**5**) and tris(6,6′-bis[8-hydroxy-3,6-dioxaoctyl-1-oxy]-3,3′-bipyridazine)ruthenium(II) dichloride (**6**) by BXV^{4+} were examined. The latter two photosensitizers lack the alkoxyanisyl binding sites and are not capable of forming supramolecular assemblies. For both photosensitizers **5** and **6**, linear Stern−Volmer luminescence plots are observed. This is exemplified in Figure 1 (curve d) with the luminescence quenching plot of **6** by BXV^{4+}. These results clearly imply that the electron-transfer quenching of the Ru(II)−bipyridazines **1**−**3** by bipyridinium salt **4** exhibits a complex route, where the electron-transfer quenching of **5** and **6** is diffusionally controlled. As the complexes **1**−**3** include the alkoxyanisyl binding sites for BXV^{4+}, the nonlinear luminescence quenching could be assigned to the formation of intermolecular photosensitizer/electron acceptor complexes. Luminescence quenching within the supramolecular assembly and via diffusional quenching of noncomplexed photosensitizer units could give rise to the nonlinear features of the Stern−Volmer plots (*vide infra*).

Further insight into the electron transfer quenching of the Ru(II)−bipyridazine complexes **1**−**3** by BXV^{4+} is gained by time-resolved laser flash photolysis experiments. Figure 2a shows the transients of the luminescence decay of **2a** by BXV^{4+}. The luminescence transients reveal two important features: (i) the initial luminescence intensity decreases as the concentration of BXV^{4+} increases, and (ii) the luminescence lifetime is shortened as the concentration of BXV^{4+} increases. These features appear to be general for the luminescence transients of

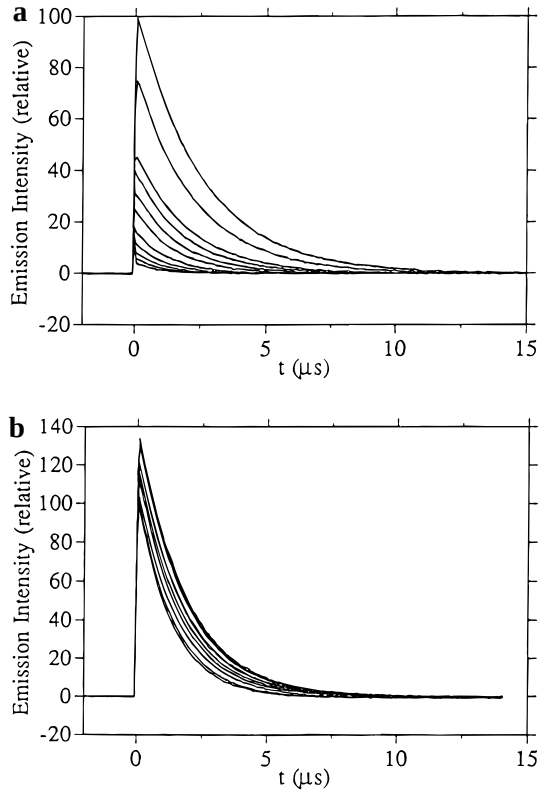

Figure 2. Transient luminescence intensities of (a) **2a** and (b) **6** in the presence and absence of BXV^{4+}. Upper transients correspond to the photosensitizer luminescence without BXV^{4+}. All other transients represent the system with added BXV^{4+} at consecutive increments corresponding to 7×10^{-4} M.

photosensitizers **1**−**3** upon addition of BXV^{4+}. The extent of decrease in the initial luminescence intensities and the shortening of the lifetimes is variable and depends on the structure of the complex and the nature of electron acceptor. Figure 2b shows the luminescence transients obtained upon addition of BXV^{4+} to the reference complex, **6**. The initial luminescence intensity remains nearly constant, but the luminescence lifetime is shortened upon increase of BXV^{4+} concentration. These features are also characteristic of the luminescence quenching of **5** by BXV^{4+}. The latter behavior, where only the luminescence lifetime is shortened upon addition of BXV^{4+}, is characteristic of a diffusional electron-transfer quenching. Thus, the unique features observed for the luminescence decay of the photosensitizers **1**−**3** by BXV^{4+} and reflected by the decrease of luminescence intensity and shortening of the lifetime are attributed to the participation of two complementary electron-transfer quenching pathways. Photosensitizers **1**−**3** including the alkoxyanisyl binding sites form supramolecular complexes with BXV^{4+}. Intramolecular electron-transfer quenching in the supramolecular assembly is fast, and reflected in the decrease of luminescence intensity (this rapid decay will be discussed and analyzed later, *vide infra*). The transient luminescence and its lifetime shortening are attributed to free photosensitizer which is quenched by the electron acceptor (BXV^{4+}) via a diffusional route, similar to that occurring in the reference compounds **5** and **6**.

To analyze quantitatively the electron-transfer quenching of photosensitizers **1**−**3** by the bipyridinium electron acceptor and to determine the association constants of the resulting supramolecular assemblies, we formulate a comprehensive model. The Ru(II)-bipyridazine complexes **1**, **2**, and **3** differ in the number of alkoxyanisyl sites ($N = 2$, 6, and 3, respectively). The kinetic model takes into consideration the photoprocesses of the

multireceptor photosensitizer, S, in the presence of the electron acceptor, A, within the resulting supramolecular assemblies exhibiting all the possible stoichiometries: SA, SA_2, ..., SA_N (N is the number of binding sites on the photosensitizer), as well as the quenching of the photosensitizer by a diffusional route. The photosensitizer configurations are generally represented as SA_n ($n = 0, 1, 2, ..., N$), where the case $n = 0$ designates the unbound photosensitizer. The relevant processes, species, and kinetic constants involved in the photoreactions of the different supramolecular photosensitizer states are summarized in eqs 1−9. These equations represent the following processes: (1) association and dissociation of the photosensitizer and electron acceptor in the ground state; (2) photoexcitation; (3) association and dissociation of the photosensitizer and acceptor in the excited state; (4) natural decay of the photosensitizer; (5) diffusional electron-transfer quenching; (6) static electron-transfer quenching within the supramolecular assemblies; (7) diffusional back electron transfer of the photogenerated redox products; (8) static back electron transfer recombination of the redox products within the supramolecular assemblies; and (9) escape or dissociation of the reduced acceptor from the supramolecular assemblies.[22]

$$SA_{n-1} + A \underset{k_{-n}}{\overset{k_n}{\rightleftharpoons}} SA_n \qquad (n = 1, 2, ..., N) \tag{1}$$

$$SA_n \xrightarrow{h\nu} S^*A_n \qquad (n = 0, 1, 2, ..., N) \tag{2}$$

$$S^*A_{n-1} + A \underset{k^*_{-n}}{\overset{k^*_n}{\rightleftharpoons}} S^*A_n \qquad (n = 1, 2, ..., N) \tag{3}$$

$$S^*A_n \xrightarrow{k_{Dn}} SA_n \qquad (n = 0, 1, 2, ..., N) \tag{4}$$

$$S^*A_n + A \xrightarrow{k_{dqn}} S^+A_n + A^- \qquad (n = 0, 1, 2, ..., N) \tag{5}$$

$$S^*A_n \xrightarrow{k_{sqn}} S^+A^-A_{n-1} \qquad (n = 1, 2, ..., N) \tag{6}$$

$$S^+A_n + A^- \xrightarrow{k_{dr}} SA_n + A \qquad (n = 0, 1, 2, ..., N) \tag{7}$$

$$S^+A^-A_{n-1} \xrightarrow{k_{sr}} SA_n \qquad (n = 1, 2, ..., N) \tag{8}$$

$$S^+A^-A_{n-1} \xrightarrow{k_{esc}} S^+A_{n-1} + A^- \qquad (n = 1, 2, ..., N) \tag{9}$$

The main assumptions adopted in the kinetic model can be summarized as follows: (a) The association rate constant is proportional to the number of free binding sites. That is, $k_n = (N + 1 - n)k_+$, where k_+ is the association constant attributed to one binding site. (b) The dissociation rate constant is proportional to the number of bound acceptor units. That is, $k_{-n} = nk_-$, where k_- is the dissociation rate constant of a single bound acceptor unit. (c) Diffusional quenching is faster than association; that is, $k_{dq} >> k^*_n$. (d) Static quenching is faster than dissociation, that is, $k_{sq} >> k^*_{-n}$. (e) All the populations of excited photosensitizer, S^*A_n ($n = 0, 1, 2, ..., N$), have the same natural decay rate constant, $k_{Dn} = k_D$. (f) All the populations of excited photosensitizers have the same diffusional quenching rate constant, $k_{dqn} = k_{dq}$. (g) The static quenching rate constant is proportional to the number of bound acceptor units, that is, $k_{sqn} = nk_{sq}$, where k_{sq} is the static quenching rate constant attributed to one acceptor unit. (h) The concentration of the acceptor is much higher as compared to the concentration of the photosensitizer, [A] >> [S]. Assumptions (a) and (b) imply that any interactions between acceptor units bound to different binding sites are neglected. Assumptions (c) and (d) imply that electron transfer is faster than the dynamics of formation or dissociation of the supramolecular complexes. That is, there is no exchange between populations of excited photosensitizer (eq 3), implying that each population of excited photosensitizer decays at a specific rate, regardless of the decays of the other populations. Assumptions (e) and (f) are less important, since the natural decay and the diffusional quenching are much slower than static quenching and, hence, are only relevant to the unbound photosensitizer. Assumption (h) means that the concentration of the acceptor is not significantly changed in the presence of the photosensitizer, and can be regarded as a constant. As a result of these assumptions (see detailed development in the Appendix), we obtain that all the concentrations of the ground-state photosensitizer and photosensitizer−acceptor assemblies, SA_n, which are found in equilibrium before photoexcitation, are given by eq 10, where S_o is the analytical concentration of the photosensitizer and $K = k_+/k_-$ is an equilibrium association constant attributed to the binding of one acceptor unit to a single binding site associated with the photosensitizer.

$$[SA]_n = \frac{S_0}{(1 + K[A])^N} \cdot \frac{N!}{n!(N-n)!} K^n [A]^n \qquad (n = 0, 1, 2, ..., N) \tag{10}$$

This is a binomial distribution which can be represented by the typical form of eq 11, where P_n is the probability of a photosensitizer to be associated to n quencher units, and $p = K[A]/(1 + K[A])$ is the probability of one binding site to be bound to an acceptor unit.

$$P_n(p) = \frac{N!}{n!(N-n)!} p^n (1-p)^{N-n} \tag{11}$$

Upon pulse irradiation of the system, equal fractions of every population are photoexcited to the excited states, S^*A_n, and immediately after excitation their population is similar to the ground-state distribution. As each population decays at a different rate, the overall decay of the luminescence of the photosensitizer is multiexponential. The transient emission decay according to this model is given by eq 12.

$$I(t) = I(0) e^{-(k_D + k_{dq}[A])t} \left(\frac{1 + K[A] e^{-k_{sq} t}}{1 + K[A]} \right)^N \tag{12}$$

Since the static quenching is much faster than the diffusional quenching ($k_{sq} >> k_{dq}[A]$), the transient luminescence is composed of a fast decay which is attributed to the static quenching in the supramolecular assemblies, SA_n ($n = 1, 2, ..., N$), and a slow decay is attributed mainly to natural decay and diffusional quenching of the unbound photosensitizer, S. The fast decay ends when the term $K[A] \exp(-k_{sq}t)$ in eq 12 becomes negligible, and then the slow emission, $I_{slow}(t)$, is expressed by eq 13.

(22) One reviewer suggested an electron exchange mechanism as an additional possible pathway for the formation of separated photoproducts:

$$S^+A^-A_{n-1} + A \xrightarrow{k_{ex}} S^+A_n + A^-$$

The major conclusion is, however, that no unbound photoproducts originating from the supramolecular assembly are detected (even at high BXV^{4+} concentrations). Hence, this process has little or no physical contribution to the electron transfer in the systems.

$$I_{slow}(t) = I(0)\frac{1}{(1 + K[A])^N} e^{-(k_D + k_{dq}[A])t} \quad (13)$$

The emission transients shown in Figure 2a are assigned to the slow emission decay, $I_{slow}(t)$, of the free photosensitizer (eq 13). The apparent decrease in the initial luminescence as the concentration at the acceptor BXV^{4+} is increased is attributed to the fast static quenching (not seen on this time scale) of higher fractions of bound photosensitizer, and the accompanying shortening of the luminescence lifetime is interpreted as a result of the diffusional quenching of the free photosensitizer (the fast decay due to static quenching was observed in complementary experiments performed at shorter time scales, which we shall describe in detail later in this paper). The emission transients corresponding to the luminescence decay of the photosensitizer including 6 alkoxyanisyl groups (**2a**) with addition of BXV^{4+} (Figure 2a) is characterized by this apparent decrease in the initial intensity, whereas the emission transients corresponding to the luminescence decay of the reference photosensitizer lacking the alkoxyanisyl groups (**6**) with addition of BXV^{4+} (Figure 2b) are only characterized by a shortening of the lifetime with almost no change in the initial intensity. This is attributed to a significant value of the association constant K for the binding of BXV^{4+} to the alkoxyanisyl group, and an almost nil value of the constant K for the binding of BXV^{4+} to the triethylene glycol chain lacking the alkoxyanisyl group.

The steady-state luminescence intensity of the photosensitizer at any concentration of electron acceptor is proportional to the integration over time of the transient luminescence intensity (eq 12) as given by eq 14, where α is a proportionality constant.

$$I = \alpha\int_0^\infty I(0)e^{-(k_D + k_{dq}[A])t}\left(\frac{1 + K[A]e^{-k_{sq}t}}{1 + K[A]}\right)^N dt \quad (14)$$

Since the term $K[A]\exp(-k_{sq}t)$ very quickly becomes null, it does not contribute significantly to the integration. That is, the steady state luminescence comes almost exclusively from the free photosensitizer. Then eq 14 can be approximated to eq 15, where τ is the lifetime of the slow luminescence decay given by eq 16.

$$I = \frac{\alpha I(0)\tau}{(1 + K[A])^N} \quad (15)$$

$$1/\tau = k_D + k_{dq}[A] \quad (16)$$

The nonlinear Stern−Volmer plots in Figure 1 (curves a, b, and c) can be rationalized by eq 17, where I_o and τ_o are the steady state luminescence intensity and the slow luminescence decay, respectively, of the photosensitizer in the absence of electron acceptor.

$$\frac{I_o}{I} = (1 + K[A])^N\frac{\tau_o}{\tau} \quad (17)$$

The Stern−Volmer plot in Figure 1 corresponding to the reference compound (**6a**) which lacks the alkoxyanisyl groups is linear since $1/\tau$ is linear (eq 16) and K is virtually null.

Figure 3 shows the shortening of the lifetimes of the photosensitizers **2a** and **6** upon addition of different concentrations of BXV^{4+} (**4**) obtained by exponential regression of the transients shown in Figure 2. According to eq 16, the diffusional quenching rate constants of **2a** and **6** by BXV^{4+} obtained from the slope of the linear regression correspond to $k_{dq} = 1.1 \times 10^8\ M^{-1}\cdot s^{-1}$ and $k_{dq} = 3.2 \times 10^7\ M^{-1}\cdot s^{-1}$, respectively. Similar analyses were performed for **1** and **3** and the reference compound **5**. Table 1 summarizes the natural decay lifetimes of the series of photosensitizers and the respective values for the diffusional electron-transfer quenching rate constant by BXV^{4+}, k_{dq}. The diffusional quenching rate constants of **1** and **2a** are comparable to those of the reference compounds **5** and **6**, respectively, albeit the values for the alkoxyanisyl complexes are slightly higher. The differences are attributed to different diffusion coefficients of the alkoxyanisyl photosensitizers, as compared to the hydroxyl-substituted reference compounds.

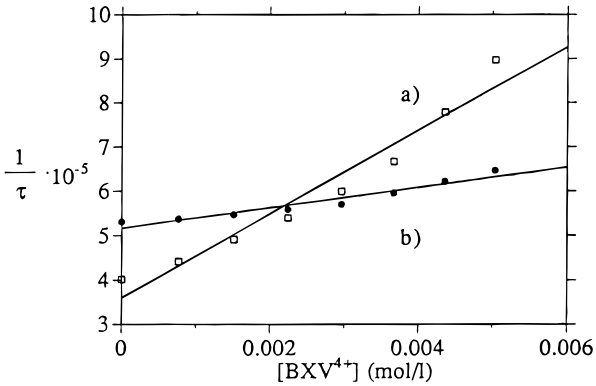

Figure 3. Shortening of the lifetime of the slow luminescence decay at different concentrations of BXV^{4+}: (a) **2a**, (b) **6**. Data of lifetimes were extracted from Figure 2.

Table 1. Diffusional and Static Electron-Transfer Quenching Rate Constants in the Photosensitizer−BXV^{4+} Assemblies and the Association Constants of the Resulting Supramolecular Systems

complex	$10^6\tau_0$ (s^{-1})	$10^{-8}k_{dq}$ ($M^{-1}\cdot s^{-1}$)[a]	K (M^{-1})[b]	$10^{-7}k_{sq}$ (s^{-1})[c]
1	2.3	1.2	240 ± 15	
2a	2.5	1.1	100 ± 10 (85)	25.0
2b	2.4	1.2	100 ± 10 (90)	4.5
3	2.4	1.2	140 ± 15	
5	2.1	0.27		
6	1.9	0.32		

[a] Deduced from the shortening of the slow-decay luminescence lifetimes. [b] Derived from the modified Stern−Volmer plots, according to eq 18. The association constants derived by analysis of the fast luminescence decay, according to eq 12, are in parentheses. [c] Derived by fitting the fast luminescence decay according to eq 12.

The association parameters and the nature of supramolecular assemblies formed between the series of photosensitizers **1**−**3** and BXV^{4+} can be analyzed by rearrangement of eq 17 in the form of a modified Stern−Volmer equation, eq 18, where I_o/I is the normal Stern−Volmer plot (as in Figure 1) obtained from steady-state measurements, and τ_o/τ is derived from the experimental values of the lifetimes, as shown in Figure 3. Figure 4 shows the modified Stern−Volmer plot of the experimental data corresponding to the electron-transfer quenching of the photosensitizer (**2a**) by BXV^{4+}, assuming maximal stoichiometries $N = 1$ (Figure 4a) and $N = 2$, 3, and 6 (Figure 4b). The best linear fitting ($R = 0.990$) is obtained for the maximal stoichiometry $N = 6$. The meaining of the plot corresponding to $N = 1$ (Figure 4a) is the molar ratio between the band and free photosensitizer. Figure 5 shows the modified Stern−Volmer plots corresponding to the electron-transfer quenching of the series of photosensitizers **1**, **2a**, and **3** by

(23) For the calculation of the second-order back electron transfer rate constants, the extinction coefficient of BXV^{3+} was assumed to be similar to that of benzyl viologen radical cation ($\epsilon = 12\ 700\ M^{-1}\cdot cm^{-1}$). The direct determination of the $BXV^{\bullet 3+}$ extinction coefficient is difficult due to the intramolecular dimerization of the radical cations of the two bipyridinium units of **4**.

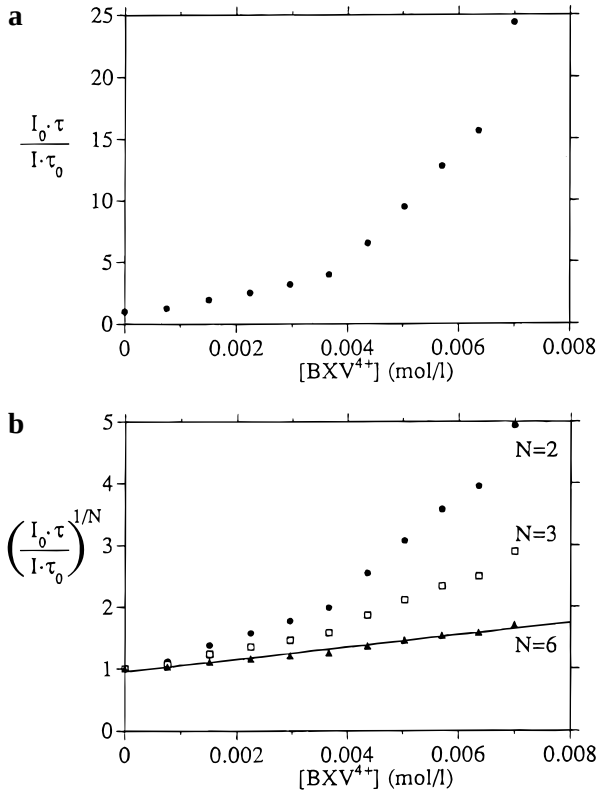

Figure 4. Modified Stern−Volmer plots for the luminescence quenching of **2a** by BXV^{4+} assuming different supramolecular maximal stoichiometries (a) $N = 1$ and (b) 2, 3, or 6. Linear fitting is observed only for $N = 6$ ($R = 0.990$).

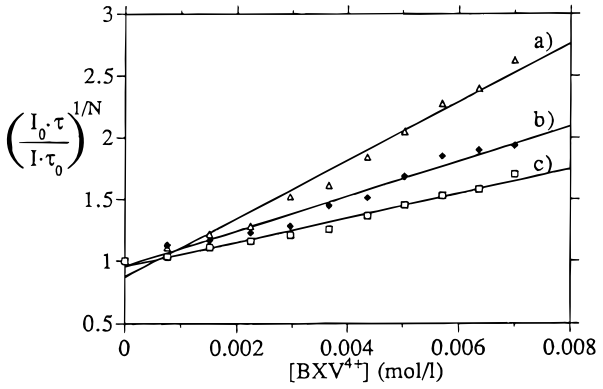

Figure 5. Modified Stern−Volmer plots for the luminescence quenching of the different photosensitizers by BXV^{4+} assuming the appropriate supramolecular maximal stoichiometries: (a) **1**, $N = 2$; (b) **3**, $N = 3$; and (c) **2a**, $N = 6$.

BXV^{4+} assuming the maximal supramolecular stoichiometries $N = 2$, 6, and 3, respectively ($R = 0.989$, 0.990, and 0.986, respectively). Thus, the best linear fittings of the modified Stern−Volmer plots for the photosensitizers **1**, **2a**, **2b**, and **3** are obtained for the supramolecular photosensitizer−BXV^{4+} stoichiometries corresponding to 2, 6, 6, and 3, respectively. It should be noted that our model and results do not imply that these are the only stoichiometries of the supramolecular photosensitizer−BXV^{4+} complexes, but the experimental results fit best upon assuming a contribution of a population of maximal binding occupancy of the photosensitizer. For example, for complex **2a** the supramolecular assembly consisting of BXV^{4+} associated to all six binding sites of the photosensitizer participates in the decay of the excited state, and other supramolecular complexes of lower stoichiometries simultaneously contribute to the decay of the excited state.

$$\left(\frac{I_o}{I}\cdot\frac{\tau}{\tau_o}\right)^{1/N} = 1 + K[A] \qquad (18)$$

The optimized association constants for the binding of the electron acceptor BXV^{4+} to a single alkoxyanisyl site in each of the complexes, deduced from the modified Stern−Volmer plots, are summarized in Table 1. It can be seen that the association constants are comparable but their values decrease as the number of binding sites in the photosensitizer increases. This might be attributed to the steric crowdedness of the binding sites in the photosensitizers containing enriched alkoxyanisyl binding sites. The analysis reveals, however, an unexpected feature of the resulting supramolecular complexes between the series of photosensitizers **1**−**3** and BXV^{4+}, where maximum binding of the quencher to the alkoxyanisyl sites is feasible. Association of BXV^{4+} to a single photosensitizer site is expected to yield electrostatic repulsive interactions for binding of the subsequent BXV^{4+} electron acceptor. The excellent fitting between the experimental data and the suggested model for electron transfer quenching in the supramolecular assemblies implies that maximum occupation of the alkoxyanisyl binding sites by BXV^{4+} is feasible. That is, the photosensitizers that include two, three and six binding sites, **1**, **3**, and **2**, form supramolecular complexes exhibiting stoichiometries of up to $N = 2$, 3, and 6, respectively.

Our discussion attributed the decrease in the initial luminescence intensities of the transients of **1**−**3** upon addition of BXV^{4+} to a fast electron-transfer quenching of the excited photosensitizer in the supramolecular assembly, S^*A_n, eq 6. Using a short-pulse laser, the fast decay of the excited photosensitizer in the supramolecular complex could be resolved. Figure 6A (curve b) shows the transient corresponding to the fast decay of photosensitizer **2a** upon addition of BXV^{4+}, where Figure 6B (curve b) shows the fast decay of photosensitizer **2b** upon addition of BXV^{4+}. For comparison, the emission profiles of **2a** and **2b** in the absence of BXV^{4+} are also provided in the respective figures (curves (a) in Figures 6A and 6B). On this short time scale no decay of the emission is observed in the absence of added BXV^{4+}, implying that the fast decay corresponds to effective electron-transfer quenching within the supramolecular assemblies. It should be noted that the fast emission intensity does not decay to zero, but to a constant finite value. This residual luminescence, which appears constant at this time scale, represents the diffusional electron-transfer quenching of the free photosensitizer by BXV^{4+} and decays to zero at a longer time window (*vide supra*). It should be noted that addition of BXV^{4+} to the reference photosensitizer **6** did not result in any fast decay at this time scale and the luminescence intensity of **6** is almost identical in the absence or presence of BXV^{4+}. This indicates that no supramolecular complexes between **6** and BXV^{4+} are formed, and no intramolecular electron transfer takes place. Photosensitizer **6** is quenched by a diffusional pathway that is observable only at a longer time scale.

The fast emission transients shown in Figure 6, corresponding to the static electron-transfer quenching within the supramolecular assemblies, were analyzed by least-squares fitting to eq 12, where the term $\exp\{-(k_D + k_{dq}[A])t\}$ was obviated (as there is no significant natural decay nor diffusional quenching at this short time scale). The parameters $I(0)$, $K[A]$, and k_{sq} were optimized. The fitted curves (overlaid in Figure 6) were in excellent agreement with the experimental points. Table 1 summarizes the resulting values of k_{sq} and K (in parentheses) derived from the least-squares fitting. The values obtained for K from these analyses are also in good agreement with the values obtained from the modified Stern−Volmer plots.

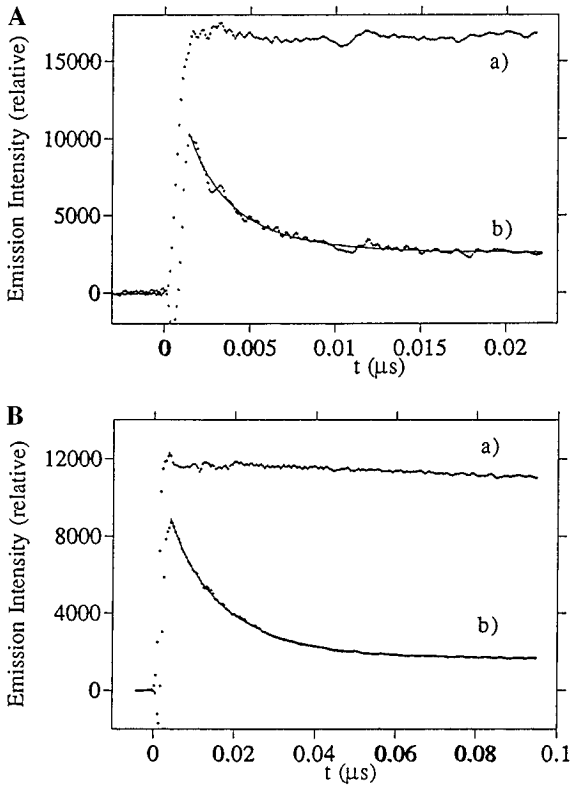

Figure 6. Transient luminescence decay corresponding to intramolecular electron-transfer quenching within the supramolecular assemblies: (A) (a) Luminescence decay of **2a**, 4.0×10^{-5} M; and (b) luminescence decay of **2a**, 4.0×10^{-5} M, in the presence of BXV^{4+}, 4.36×10^{-3} M. (B) (a) Luminescence decay of **2b**, 4.0×10^{-5} M and (b) luminescence decay of **2b**, 4.0×10^{-5} M in the presence of BXV^{4+}, 4.36×10^{-3} M.

It is interesting to note that the intramolecular electron-transfer-quenching rate constant of **2a** by BXV^{4+} is ca. 5 times faster than that of **2b**. The two photosensitizers differ by a single ethylene glycol unit in the tether chain bridging the alkoxyanisyl binding site to the photosensitizer. We can assume that formation of the supramolecular assemblies between the BXV^{4+} electron acceptor and the photosensitizers results in electrostatic repulsive interaction as well as steric hindrance that stretch the diad assemblies. The longer electron transfer distance in photosensitizer **2b**, as a result of the longer tether bridge, decreases the intramolecular quenching rate constant as compared to **2a**. A similar effect of the tether length is observed in the back electron transfer of the redox photoproducts (*vide infra*).

We thus conclude that the series of photosensitizers **1**−**3** form an equilibrium mixture of free photosensitizer and mono- and polydentate supramolecular photosensitizer−acceptor diads. Figure 7 shows schematically the various supramolecular assemblies formed between **3** and BXV^{4+}. Quantitative analysis of the electron-transfer quenching of the series of photosensitizers implies that multisubstitution of the alkoxyanisyl sites by BXV^{4+} occurs despite the electrostatic repulsions between BXV^{4+} units. We believe that stabilizing donor−acceptor interactions and the length of the flexible tether bridging chains compensate for the electrostatic repulsive interactions.

Finally, we examined the electron-transfer products formed upon quenching via the intramolecular pathway in the supramolecular complexes and by the diffusional route where the free photosensitizer is quenched. Figure 8 shows the transient of the photoreduced product $BXV^{\bullet 3+}$ formed upon excitation of **2a**. It exhibits a characteristic absorbance at $\lambda = 600$ nm. The decay of the reduced product corresponds to the recombination process. The decay does not fit a first- or second-order reaction over the entire time domain. The transient, however, can be separated into a fast recombination which follows a first-order kinetics and to a slow recombination that follows a second-order kinetics. The fast first-order decay is attributed to back electron transfer from the bound reduced acceptor, $BXV^{\bullet 3+}$, to the oxidized chromophore, within the supramolecular assembly (eq 8). The slow second-order decay is attributed to the diffusional back electron transfer between the reduced acceptor and an oxidized photosensitizer which are not associated (eq 7). The rate constants of the static and diffusional back-electron-transfer recombination of the photoproducts formed upon quenching of **2a** by BXV^{4+}, which are obtained from first-order analysis of the fast decay and second-order analysis of the slow decay of the absorption of $BXV^{\bullet 3+}$, are $k_{sr} = 1.8 \times 10^6\ s^{-1}$ and $k_{dr} = 3.5 \times 10^9\ M^{-1}\cdot s^{-1}$, respectively.

A similar behavior is observed for the series of Ru(II)−bipyridazine complexes that include the alkoxyanisyl units, **1**−**3**, Table 2. That is, for all these Ru(II) photosensitizers, the formation of the supramolecular complexes with BXV^{4+} results in two distinct populations of photoproducts: the supramolecular complex composed of the reduced and oxidized products, where back electron transfer proceeds by a first-order kinetics, k_{sr}, eq 8. The second population of photoproducts corresponds to free redox intermediates, eq 7, that recombine via a second-order process, k_{dr}. Table 2 summarizes the intramolecular and diffusional back electron transfer rates in the series of complexes **1**−**3**. The back electron transfer of the photogenerated redox products formed by quenching of the reference photosensitizer (**6**) lacking the alkoxyanisyl binding groups was exclusively second order, a fact that provides further evidence that the alkoxyanisyl groups are responsible for the formation of the supramolecular assemblies.

Another important aspect to note about the analysis of the back electron transfer is the relative contribution of the fast first-order static component and the slow second-order diffusional component. If the reduced bound acceptor, formed upon static quenching within the supramolecular assembly, does not dissociate (eq 9) before the back electron transfer occurs, then we should expect the ratio between the photoproduct populations undergoing static and diffusional back electron transfer to be equal to the ratio between the photosensitizer populations undergoing static and diffusional quenching. If, otherwise, the reduced acceptor formed upon static quenching escapes from the supramolecular assembly, then the ratio between photoproduct populations undergoing static and diffusional back electron transfer should decrease as compared to the respective populations of quenched photosensitizer. Table 2 shows the fraction of photosensitizer undergoing static quenching (θ_{sq}) and the fraction of photoproducts undergoing static back electron-transfer recombination (θ_{sr}). We see that for photosensitizers **1** and **3** there is no significant difference between θ_{sr} and θ_{sq}. For complexes **2a** and **2b**, θ_{sr} is slightly higher than θ_{sq}. Since the difference is not much larger than the error range, we can only give an upper limit to the escape efficiency, $\theta_{esc} = k_{esc}/(k_{sr} + k_{esc})$, or $(\theta_{sr} - \theta_{sq})/\theta_{sq} = 0.08$. That is, not more than 8% of the reduced acceptor formed upon electron transfer within the supramolecular assembly succeeds in escaping from back electron transfer within the supramolecular assemblies. We could expect, in principle, that the dissociation of a reduced acceptor unit (which has lesser π-acceptor character) should be faster than the dissociation of an unreduced acceptor unit ($k_{esc} > k_{-n}, k^*_{-n}$), and hence the escape of the reduced photoproducts should be feasible. We note, however, that the acceptor BXV^{4+}

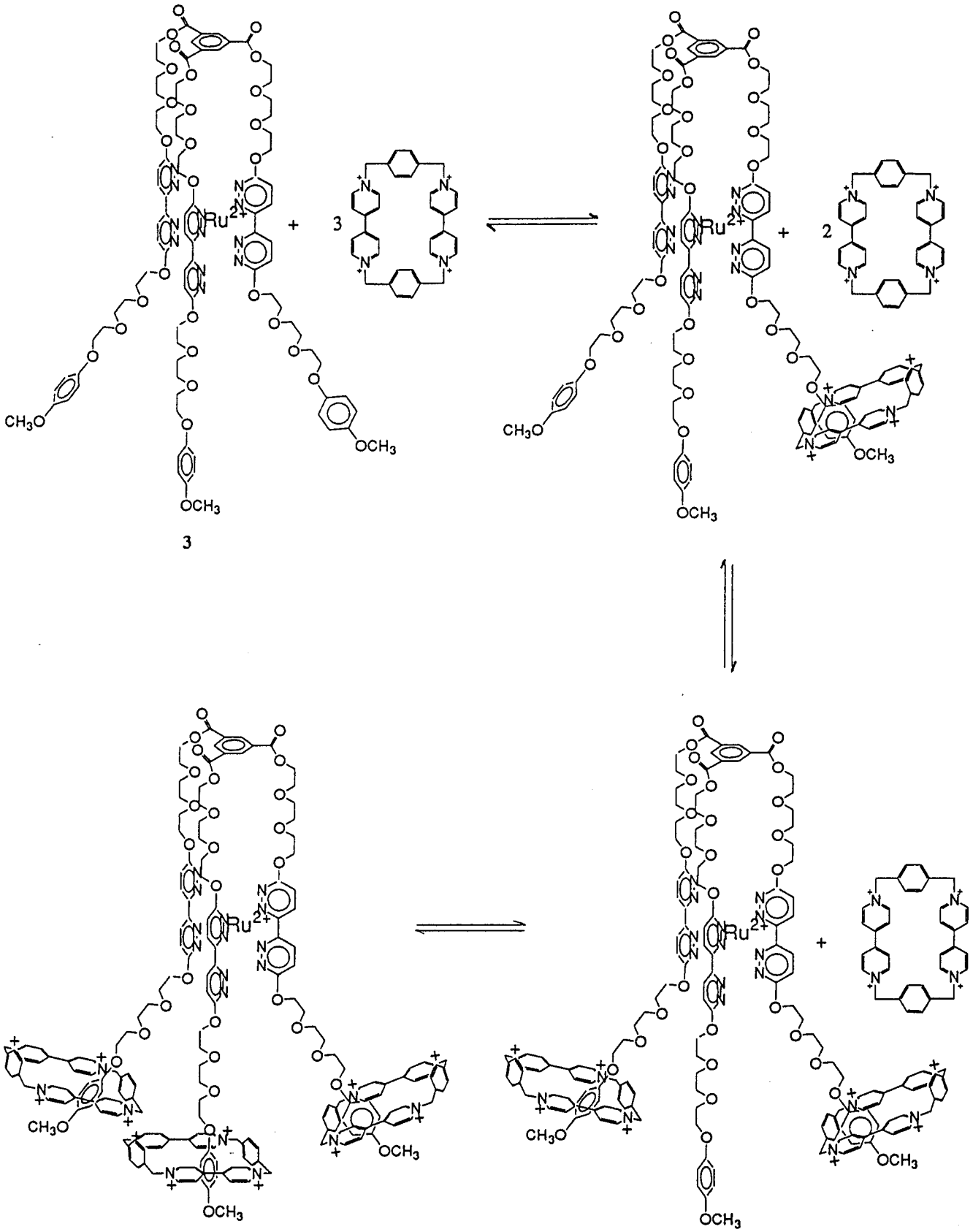

Figure 7. Scheme for the equilibrated supramolecular assemblies formed between **3** and BXV^{4+}.

is composed of two non-conjugated bipyridinium moieties, and only one of them is reduced, while the other one is still capable of forming a π-donor−acceptor complex with the alkoxyanisyl group. The relatively stable supramolecular structures even after electron transfer are attributed to the stabilization of π-donor−acceptor complexes between the alkoxyanisyl units and the oxidized bipyridinium sites of $BXV^{\bullet 3+}$. Thus, the non-covalently linked supramolecular assemblies SA_n act as static diads where electron-transfer quenching and recombination occurs in intact supramolecular structures despite the dynamic nature of the systems.

The reference compounds **5** and **6** that do not form supra-

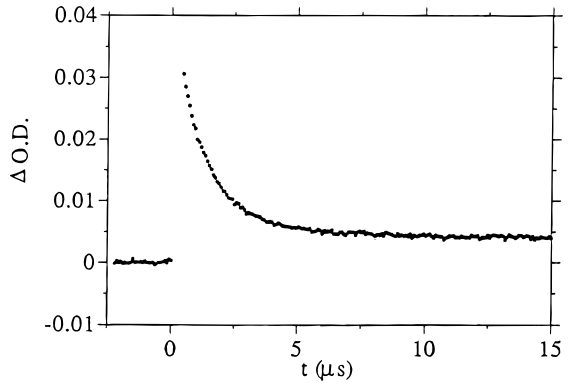

Figure 8. Transient decay of the reduced photoproduct, $BXV^{\bullet 3+}$ formed upon excitation of **2a**, as a result of back electron transfer. Reduced photoproduct was followed at $\lambda = 600$ nm.

Table 2. Diffusional and Static Back Electron Transfer Rate Constants and Fraction of Photosensitizer or Redox Photoproducts Being Quenched or Undergoing Recombination by the Intramolecular Pathways

photosensitizer	$10^{-6}k_{sr}$ (s^{-1})[a]	$10^{-9}k_{dr}$ ($M^{-1}\cdot s^{-1}$)[b]	θ_{sq}[c]	θ_{sr}[d]
1	0.83	5.9	0.71	0.70
2a	1.76	3.5	0.85	0.78
2b	0.87	3.4	0.84	0.78
3	0.96	5.6	0.71	0.74
5		2.2	≈0	≈0
6		1.2	≈0	≈0

[a] Determined by analysis of the fast decay absorption transient of $BXV^{\bullet 3+}$. [b] Determined by analysis of the slow decay absorption transient of $BXV^{\bullet 3+}$. [c] θ_{sq} correspsonds to the fraction of photosensitized being quenched by intramolecular electron transfer in the supramolecular assemblies. Values determined from the modified Stern−Volmer plots correspond to systems where $[BXV^{4+}] = 4.36 \times 10^{-3}$ M. [d] θ_{sr} corresponds to the fraction of reduced photogenerated product that recombines via intramolecular back electron transfer in the supramolecular assemblies.

molecular complexes with BXV^{4+} form upon photoexcitation the respective photoproducts that recombine via a second-order diffusional back electron transfer. The recombination rate constants for these photosensitizers are also included in Table 2.

Figure 7 shows schematically the supramolecular assemblies formed by photosensitizer **3** and the electron acceptor, BXV^{4+}. We have shown that photoinduced electron transfer occurs in the supramolecular assemblies and that the electron-transfer products are stable in the resulting structure and do not dissociate within their lifetime. The formation of the intermolecular complexes between the alkoxyanisyl Ru(II) photosensitizer and BXV^{4+} represents a novel means to generate non-covalently-linked photosensitizer−acceptor diads. It should be noted that the lifetime of the redox photoproducts $Ru^{3+}-BXV^{\bullet 3+}$ in the various systems is relatively long, 0.56−1.20 μs. This value is substantially longer than the lifetime observed in covalently linked porphyrin−quinone or Ru(II)−tris-bipyridine-bipyridinium diads. In the present systems, the alkoxyanisyl binding units, acting as the active site for assembling the photosensitizer−BXV^{4+} complexes, is tethered to the photosensitizer unit by a relatively long polyethylene bridging chain. Association of BXV^{4+} to the binding site results in electrostatic repulsive interaction between the Ru(II) photosensitizer unit and the acceptor component. These repulsive interactions stretch the bridging chain, and as a result the photogenerated redox products are spatially separated. The spatial (distance) separation imposed by the electrostatic interactions stabilizes the photoproducts against back electron transfer. This phenomenon is supported by comparison of the intramolecular back electron transfer rate constants, k_{sr}, in the supramolecular systems consisting of photosensitizers **2a** and **2b**. The two photosensitizers differ only by one ethylene glycol unit that links the alkoxyanisyl binding site to the Ru(II) photosensitizer. The intramolecular back electron transfer rate constant of the photogenerated redox products is ca. 2-fold slower in the complex formed with **2b** (see Table 2). The slower recombination rate in the supramolecular assembly **2b**−BXV^{4+} as compared to **2a**−BXV^{4+} is attributed to the longer tether linking BXV^{4+} to the photosensitizer that assists the spatial separation of the redox products.

Conclusions

We have demonstrated a novel means to organize photosensitizer−electron acceptor diad arrays by structural tailoring of the photosensitizer with electron donor groups capable of generating supramolecular diads via donor−acceptor interactions. Effective intramolecular electron transfer quenching proceeds in the resulting supramolecular assemblies. Mechanistic analysis of the intramolecular electron-transfer quenching and of the back electron transfer of the photogenerated redox products within the supramolecular systems revealed several important features: (i) The electron transfer quenching proceeds in two distinct populations of the photosensitizer that include supramolecular assemblies of the photosensitizer−acceptor components and free photosensitizer that is quenched via a diffusional pathway. (ii) For multireceptor photosensitizers, which include several binding sites for the acceptor, supramolecular assemblies of variable stoichiometries SA_n up to complete occupation of all binding sites are formed. For example, for the hexadentate photosensitizer, **2**, formation of complexes of stoichiometries SA, SA_2, ..., SA_6 is supported by mechanistic analysis of the electron-transfer quenching. Functionalization of the supramolecular photosensitizer-acceptor assembly by a high degree of electron acceptor components enhances the intramolecular electron transfer quenching. (iii) The electron transfer products formed in the systems reveal two distinct populations consisting of the redox products within the supramolecular assembly and redox products formed via diffusional quenching of free photosensitizers. The two groups of redox products are non-exchangeable within the lifetime of back electron transfer. (iv) The lifetime of the redox products in the resulting supramolecular assemblies is relatively long as compared to covalently-linked diad systems. This is attributed to the fact that the electron-acceptor binding sites are tethered to the photosensitizer by long-chain spacing bridges. Electrostatic repulsion between the electron acceptor units and the photosensitizer site results in stretched conformations of the diads. The resulting spatial separation of the redox products stabilizes them against back electron transfer.

We thus conclude that although the series of photosensitizers **1**−**3** and the electron acceptor BXV^{4+} (**4**) represent dynamic systems, the electron transfer quenching and the recombination of the photogenerated redox products proceed in static supramolecular assemblies consisting of photosensitizer−BXV^{4+}. Further modification of the primary BXV^{4+} electron acceptor with secondary electron acceptors is anticipated to yield more complex supramolecular triad assemblies where vectorial electron transfer would enhance the lifetime of the resulting redox products.

Appendix: Quenching of a Multireceptor Photosensitizer by a Quencher Substrate

We supply here the algebraic paths that lead from assumptions (a)−(h) of the kinetic model stated in the section of Results

and Discussion, to the derivation of eq 10 expressing the distribution of the electron acceptor units over the multireceptor photosensitizer units, and to eq 12 describing the after-pulse decay of the luminescence intensity in the systems.

The ground-state species SA_n ($n = 0, 1, 2, ..., N$) are found in equilibrium prior to the application of the laser pulse. According to eq 1 and to assumptions (a) and (b), the equilibrium constants can be defined by eq 19 which gives the

$$\frac{[SA_n]}{[SA_{n-1}][A]} = \frac{k_n}{k_{-n}} = \frac{(N+1-n)k_+}{nk_{-1}} \tag{19}$$

concentration of each population, SA_n, in an inductive way with respect to its precursor, SA_{n-1}. This can be cumulatively expressed by eq 20, which can be converted to eq 21, where $K = k_+/k_-$.

$$[SA_n] = [S]\prod_{i=1}^{n}\frac{(N+1-i)k_+}{ik_-}[A] \tag{20}$$

$$[SA_n] = [S]\frac{N!}{n!(N-n)!}K^n[A]^n \tag{21}$$

The analytical concentration of the photosensitizer, S_o, is the sum of the concentrations of all the populations, as given by eq 22

$$S_o = \sum_{n=0}^{N}[SA_n] = [S]\sum_{n=0}^{N}\frac{N!}{n!(N-n)!}K^n[A]^n \tag{22}$$

which can be converted by the expression of the binomium to eq 23.

$$S_o = [S](1+K[A])^N \tag{23}$$

Combining eqs 21 and 23 yields eq 10.

The distribution of the excited state immediately after photoexcitation of $[S^*A_n](0)$ is similar to that of the ground state, as given by eq 24, where S^*_o represents the overall concentration of excited state species.

$$[S^*A_n](0) = \frac{S^*_o}{(1+K[A])^N}\frac{N!}{n!(N-n)!}K^n[A]^n \tag{24}$$

According to eq 4, 5, and 6, and to assumptions (c)−(g), each population of the excited states S^*A_n follows a first-order exponential decay, given by eq 25.

$$[S^*A_n](t) = [S^*A_n](0)e^{-(k_D+k_{dq}[A]+nk_{sq})t} \tag{25}$$

The transient emission intensity is proportional to the sum of the concentration of all the excited states, eq 26.

$$\frac{I(t)}{I(0)} = \frac{1}{S^*_o}\sum_{n=0}^{N}[S^*A_n](t) \tag{26}$$

Combination of eqs 24, 25, and 26 leads to eq 27, which can be reorganized into the form of eq 28. The latter is brought, by the expression of the binomium, to the final form of eq 12.

$$I(t) = \sum_{n=0}^{N}\frac{I(0)}{(1+K[A])^N}\cdot\frac{N!}{n!(N-n)!}K^n[A]^n e^{-(k_D+k_{dq}[A]+nk_{sq})t} \tag{27}$$

$$I(t) = I(0)\frac{e^{-(k_D+k_{dq}[A])t}}{(1+K[A])^N}\sum_{n=0}^{N}\frac{N!}{n!(N-n)!}(K[A]e^{-k_{sq}t})^n \tag{28}$$

Acknowledgment. The research project is supported by the Volkswagen Stiftung. The support of the laser laboratory at The Hebrew University by the James Frank Foundation is gratefully acknowledged. The support of the DAAD program (M.K.) is acknowledged. We thank Prof. M. Ottolenghi for enabling us to use the N_2-laser system. We also express our gratitude to Mrs. V. Heleg-Shabtai for her assistance and Mr. S. Ravid (Rabinovitz) and Ms. M. Armony for their helpful discussion on the mathematical analysis of the experimental results.

JA952070P